Superhydrophilic Graphdiyne Accelerates Interfacial Mass/Electron Transportation to Boost Electrocatalytic and Photoelectrocatalytic Water Oxidation Activity

Jian Li, Xin Gao, Zhenzhu Li, Jing-Hao Wang, Lei Zhu, Chen Yin, Yang Wang, Xu-Bing Li, Zhongfan Liu, Jin Zhang, Chen-Ho Tung, and Li-Zhu Wu**

Graphdiyne (GDY), with a highly π-conjugated structure of sp^2- and sp-hybridized carbon, has triggered a huge interest in water splitting. However, all of the systems perform with no consideration of the surface wettability of GDY. Herein, for the first time, the fabrication of superhydrophilic GDY electrode via air-plasma for oxygen evolution is described. As a representative catalyst, ultrathin CoAl-LDH (CO_3^{2-}) nanosheets have been successfully assembled onto the superhydrophilic GDY electrostatically. The resulting superhydrophilic CoAl-LDH/GDY electrode exhibites superior activity with an overpotential of ≈258 mV to reach 10 mA cm^{-2}. The turnover frequency (TOF) is calculated to be ≈0.60 s^{-1} at η = 300 mV, which is the best record in both CoAl-based and GDY-based layered double hydroxides (LDH) electrocatalysts for oxygen evolution. Density functional theory (DFT) calculations reveal that superhydrophilic GDY has stronger interactions with catalysts and attracts H_2O molecules around catalysts, thus facilitating interfacial mass/electron transportation. Further, the fabrication is capable of improving the photoelectrochemical oxygen evolution activity remarkably. The results show the great potential of superhydrophilic GDY to boost water oxidation activity by promoting interfacial mass/electron transportation.

1. Introduction

Owing to the excellent electrical conductivity, remarkable stability, large surface area, and uniformly distributed pores, graphdiyne (GDY) becomes a rising star on the horizon of 2D carbon materials,[1,2] and has stimulated tremendous research interest both from theoretical prediction[3] and practical applications.[4–10] The unique π-conjugated 2D structure, consisting of sp- and sp^2-hybridized carbon atoms, has shown great potential in catalysis,[4] Li ion battery,[5] environmental remediation,[6] and renewable energy applications.[7–10] Very recently, GDY had been successfully used for electrocatalytic or photoelectrocatalytic water splitting,[8–10] a promising approach to overcome the increasing energy crisis and environmental pollutions.[11,12] However, all the systems performed with no consideration of surface wettability of GDY, a key factor to affect the interfacial microenvironment. Because the water splitting reaction takes place only at the interface of solid electrocatalyst, liquid electrolyte, and gaseous molecules,[13] judiciously engineering the interface microenvironment of working electrode with favorable mass diffusion and electron transfer is essential to promote the catalytic performance.[14] It is anticipated that the intrinsically hydrophobic GDY would make electrolyte difficult to immerse the electrode, produce dead area, and form gas pocket on the surface, thereby leading

Dr. J. Li, J.-H. Wang, L. Zhu, Y. Wang, Dr. X.-B. Li, Prof. C.-H. Tung, Prof. L.-Z. Wu
Key Laboratory of Photochemical Conversion and Optoelectronic Materials
Technical Institute of Physics and Chemistry
the Chinese Academy of Sciences
Beijing 100190, P. R. China
E-mail: lzwu@mail.ipc.ac.cn

Dr. J. Li, J.-H. Wang, L. Zhu, Y. Wang, Dr. X.-B. Li, Prof. C.-H. Tung, Prof. L.-Z. Wu
School of Future Technologies
University of Chinese Academy of Science
Beijing 100049, P. R. China

The ORCID identification number(s) for the author(s) of this article can be found under https://doi.org/10.1002/adfm.201808079.

Dr. X. Gao, C. Yin, Prof. Z. Liu, Prof. J. Zhang
Center for Nanochemistry
Beijing Science and Engineering Center for Nanocarbons
Beijing National Laboratory for Molecular Sciences
College of Chemistry and Molecular Engineering
Peking University
Beijing 100871, P. R. China
E-mail: jinzhang@pku.edu.cn

Dr. Z. Li
Soochow Institute for Energy and Materials Innovations (SIEMIS)
College of Physics
Optoelectronics and Energy & Collaborative Innovation Center of Suzhou Nano Science and Technology
Soochow University
Suzhou 215006, P. R. China

DOI: 10.1002/adfm.201808079

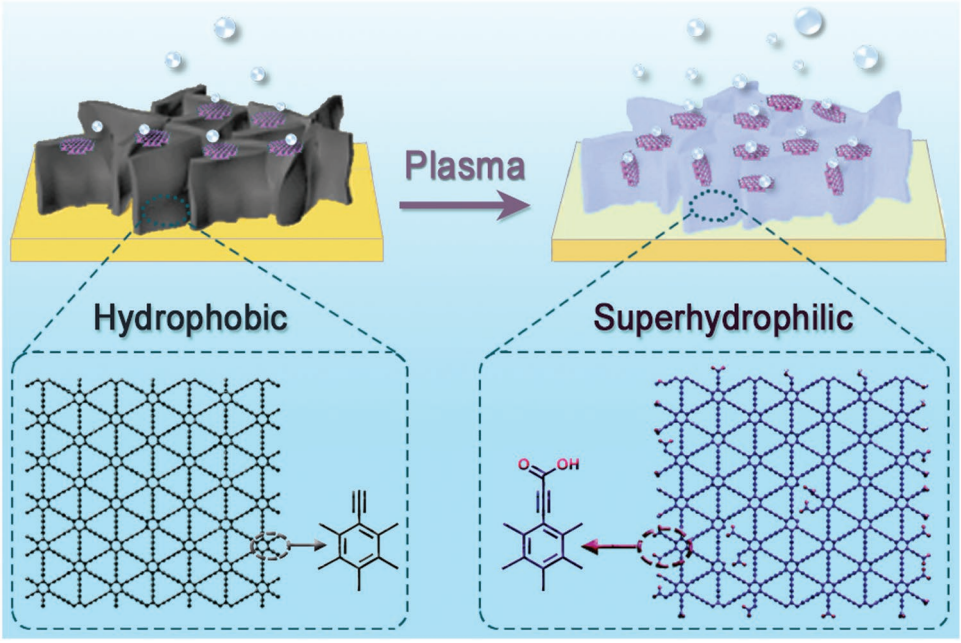

Scheme 1. Comparision of CoAl-LDH (CO_3^{2-}) assembled hydrophobic and superhydrophilic GDY electrodes.

to a decreased interfacial concentrations of reactants and an impeded mass/electron transfer process. In this situation, one may wonder whether superhydrophilic GDY electrodes could boost catalytic activity toward water splitting by right of sufficient electrode–electrolyte contact and improved interfacial mass/electron transfer.

Toward this end, we initiated the study to fabricate a superhydrophilic GDY electrode. Herein, air-plasma is used to increase hydrophilic oxygenic groups of carbon materials (such as —O—, —OH, and —COOH). Compared with conventional oxidant-treated manner, plasma can avoid destroying the substrate, which is very important to the fabrication of devices. As a representative catalyst, ultrathin CoAl (CO_3^{2-}) layered double hydroxides (LDHs) nanosheets were assembled on superhydrophilic GDY for oxygen evolution reaction (OER),[15–20] the bottleneck of water splitting (**Scheme 1**).[21,22] To our delight, the superhydrophilic CoAl-LDH/GDY showed excellent OER activity with an overpotential of ≈258 mV to reach 10 mA cm^{-2}, much better than that of hydrophobic CoAl-LDH/GDY (≈360 mV) under the same condition. The turnover frequency (TOF) on the basis of Co was determined as ≈0.60 s^{-1} at η = 300 mV, which is the best value in both CoAl-based and GDY-based LDH electrocatalysts.[15–18] Density functional theory (DFT) calculations revealed that superhydrophilic GDY exhibited a more negative charge density and could attract H_2O molecules closer to catalysts, thus facilitating interfacial mass/electron transportation efficiently (see below). Furthermore, the fabrication has been successfully extended to superhydrophilic CoAl-LDH/GDY/$BiVO_4$ photoanode, achieving a great increase in photoelectrocatalytic activity. All of the results indicate that superhydrophilic GDY is promising to overcome the sluggish kinetics and large overpotential of OER and thus greatly promotes water oxidation activity.

2. Results and Discussion

GDY was first synthesized on 3D porous Cu foam via modified Glaser–Hay coupling reaction.[2] Scanning electron microscopy (SEM) revealed that GDY possessed porous nanostructure with vertically regular cross-linked nanowalls (**Figure 1**a) and the porous structure was maintained after air-plasma treatment (Figure 1d). Static contact angles (CAs) were performed to evaluate the wettability of GDY before and after air-plasma treatment. As shown in Figure 1b,e, the surface wettability of GDY changed from hydrophobicity (CAs ≈ 139.2°) to superhydrophilicity (CAs ≈ 0°) even after 2 minutes of plasma treatment (Figure S1, Supporting Information). The change of surface wettability was ascribed to the hydrophilic oxygenic functional groups generated from oxidation of alkyne groups by air-plasma, which were confirmed by energy dispersive X-ray spectrometer (EDS; Figure S2, Supporting Information) and X-ray photoelectron spectroscopy (XPS). Figure 1c showed the high-resolution C 1s of hydrophobic GDY, which could be deconvoluted into four subpeaks at 284.5, 285.3, 286.8, and 288.6 eV, consistent with sp^2 (C=C), sp (C≡C), C—O, and C=O, respectively. The small amount of oxygen species in hydrophobic GDY stems from the adsorption of air and oxidation of some terminal alkyne.[2] In contrast, a greatly increased proportion of oxygenic groups in superhydrophilic GDY was observed (Figure 1f) and the increased oxygen species was mainly C=O group (Figure S3, Supporting Information). In the Raman spectra of superhydrophilic GDY, the acetylenic bond peaks shifted to

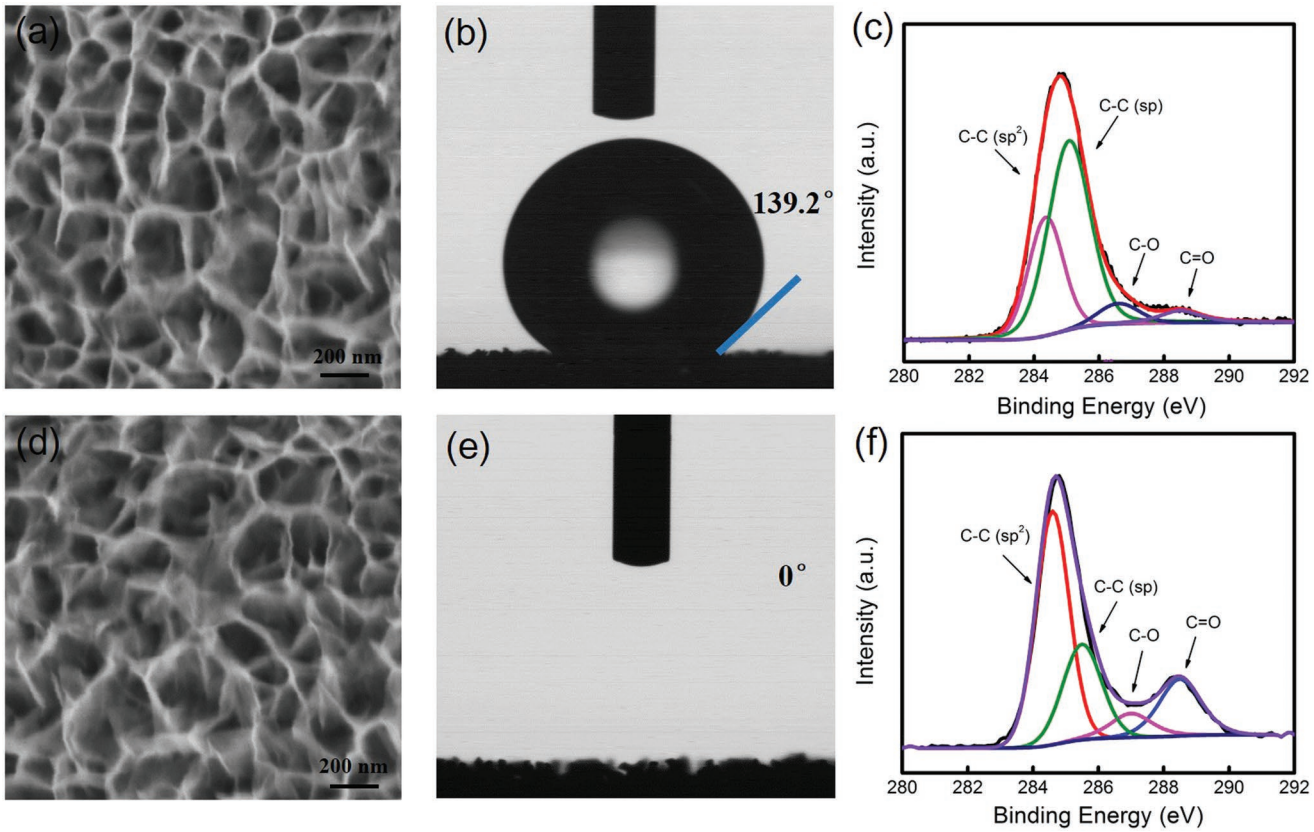

Figure 1. a,d) SEM images of GDY before and after plasma treatment; b,e) static water contact angles of GDY before and after air-plasma treatment; c,f) high-resolution XPS spectrum of C 1s for GDY before and after air-plasma treatment.

higher wavenumber with lowered intensity, further confirming some alkyne groups were oxidized to electron-withdrawing groups (Figure S4, Supporting Information).[23] All of the observations demonstrated that air-plasma treated GDY kept the basic skeleton of GDY and the introduced oxygenic groups enabled the superhydrophilicity of GDY from hydrophobicity.

The ultrathin CoAl-LDH (CO_3^{2-}) nanosheets were synthesized by a one-step hydrothermal method using ethylene glycol as reaction solvent (see Supporting Information). The low contrast in TEM image revealed the ultrathin nature (Figure S5, Supporting Information) and the thickness of exfoliated nanosheets was measured to be ≈1.7 nm by AFM (Figure S6, Supporting Information). The zeta potential around +37.5 mV (Figure S7, Supporting Information) suggested that CoAl-LDH (CO_3^{2-}) nanosheets possessed high positive charge and the small water contact angle (≈14°) showed its hydrophilic properties (Figure S8, Supporting Information). After immersing the superhydrophilic GDY into the CoAl-LDH (CO_3^{2-}) solution for 6 h, the superhydrophilic CoAl-LDH/GDY electrode was successfully prepared via electrostatic interaction between positively charged CoAl-LDH and superhydrophilic GDY. The SEM image showed that the porous structure of superhydrophilic CoAl-LDH/GDY electrode remained but its surface became much rougher (**Figure 2**a). TEM image and corresponding elemental mapping proved the uniform dispersion of C, O, Co, and Al in superhydrophilic CoAl-LDH/GDY (Figure 2b–c). A clear lattice fringe of 0.254 nm (Figure 2d), corresponding to the (012) crystalline planes of CoAl-LDH, was observed in the HRTEM image. Moreover, the signals of elemental Co and Al were also detected in the XPS spectra (Figure 2e). The high-resolution XPS spectra of Co 2p in superhydrophilic and hydrophobic CoAl-LDH/GDY displayed peak shift to higher binding energy compared to bare CoAl-LDH (CO_3^{2-}) nanosheets (Figure 2f). Notably, superhydrophilic CoAl-LDH/GDY (≈0.4 eV) showed a larger shift than hydrophobic CoAl-LDH/GDY (≈0.15 eV), indicating the stronger interaction and electronic coupling between superhydrophilic GDY and CoAl-LDH (CO_3^{2-}), which was beneficial to the electron transfer from catalyst to GDY.

Next, electrocatalytic OER activities of different samples were measured in 0.1 M KOH solution. As shown in **Figure 3**a, the hydrophobic GDY exhibited no apparent catalytic current in the test range, but the resultant superhydrophilic GDY displayed increased catalytic current. The catalytic activity increased with the processing time and reached maximum around 10 min (Figure S9, Supporting Information). More importantly, the prepared superhydrophilic CoAl-LDH/GDY electrode exhibited the highest catalytic density and the lowest overpotential. To achieve 10 mA cm^{-2}, the superhydrophilic CoAl-LDH/GDY electrode only required an overpotential of

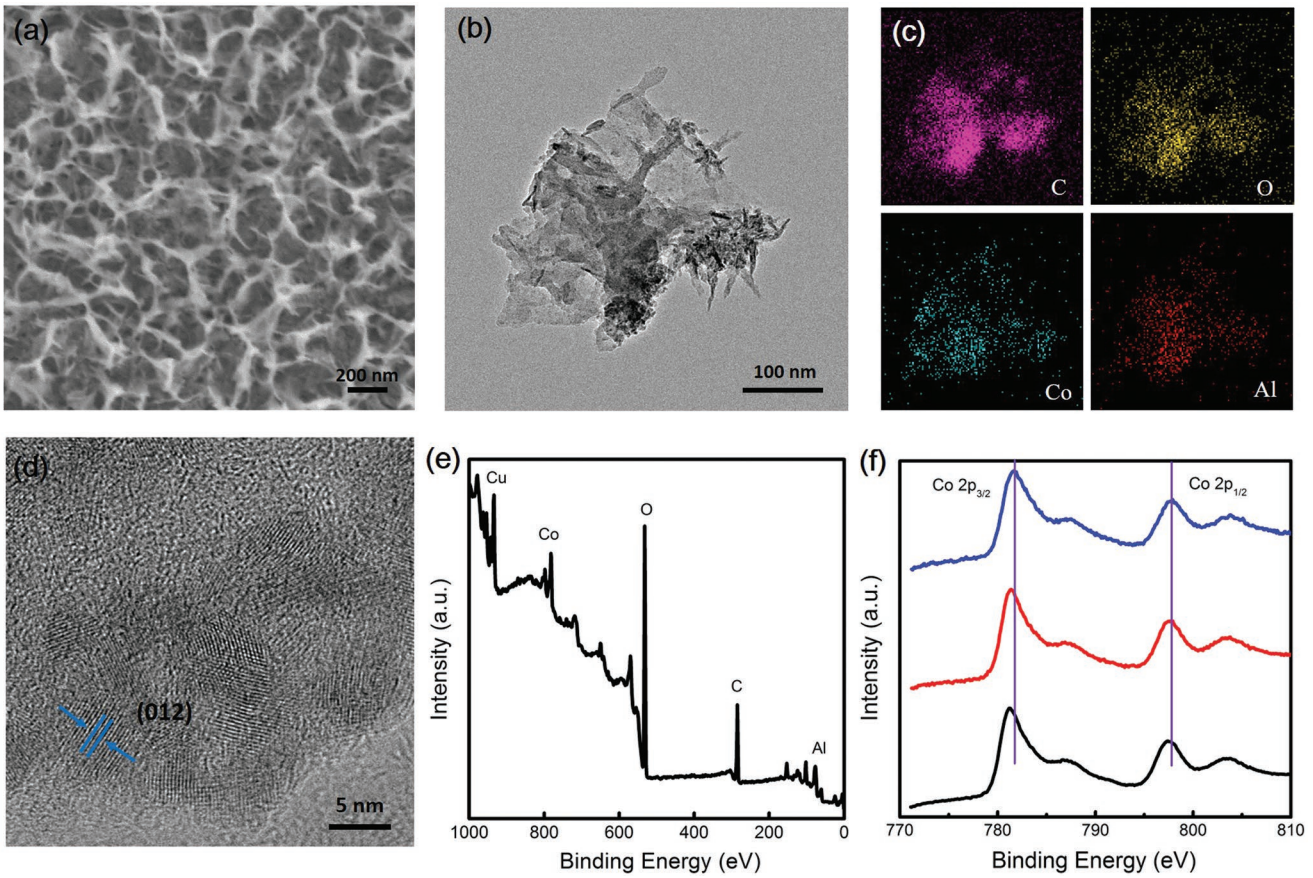

Figure 2. a) SEM image and b) TEM image of superhydrophilic CoAl-LDH/GDY electrode; c) the corresponding elemental mapping of C, O, Co, and Al; d) HRTEM image of superhydrophilic CoAl-LDH/GDY; e) full XPS spectra of superhydrophilic CoAl-LDH/GDY; f) the high-resolution XPS spectrum of Co 2p for bare CoAl-LDH (black line), hydrophobic (red line), and superhydrophilic (blue line) CoAl-LDH/GDY electrodes.

≈258 mV (Figure 3b). At the overpotential of 300 mV, the catalytic current density could reach 24.8 mA cm^{-2}. Based on the amount of catalysts on superhydrophilic GDY measured by ICP-MS (6.35 μg cm^{-2}), the TOF was calculated to be ≈0.60 s^{-1} at the overpotential of 300 mV, which is the best record in both CoAl-based and GDY-based LDH electrocatalysts,[15–18] even comparable to the best performance of LDH-based electrocatalysts for oxygen evolution (Table S1, Supporting Information). As to the hydrophobic CoAl-LDH/GDY, it required ≈360 mV to reach 10 mA cm^{-2} current density (Figure 3b) and the amount of catalysts adsorbed on hydrophobic GDY electrode was ≈4.97 μg cm^{-2}, corresponding to a TOF of ≈0.14 s^{-1} at η = 300 mV, which are poorer than those of superhydrophilic CoAl-LDH/GDY electrode. The lowest Tafel slope of ≈94 mV dec^{-1} and smallest semicircle in electrochemical impedance spectra (EIS) for superhydrophilic CoAl-LDH/GDY electrode further demonstrated the highly efficient and fast charge transfer ability for OER (Figure 3c–d). In addition, the double-layer capacitances (C_{dl}) were tested to assess the electrochemical active surface area (ECSA). According to the cyclic voltammetry (CV) curves at nonfaradic regions (Figure S10, Supporting Information), the C_{dl} of superhydrophilic CoAl-LDH/GDY was determined as ≈0.86 mF cm^{-2} (Figure 3e), much larger than those of other samples, indicating the most exposed active sites. Notably, the current density of superhydrophilic CoAl-LDH/GDY electrode at 1.50 V versus RHE showed negligible degradation during 25 h test (Figure 3f), and the corresponding faradic efficiency for oxygen was calculated as ≈95% (Figure S11, Supporting Information).

To understand the superiority of superhydrophilic GDY, DFT calculations were carried out by introducing a −COOH group in a 5 × 5 matrix of GDY to represent superhydrophilic GDY (Figure S12, Supporting Information). As shown in **Figure 4**a,b, the superhydrophilic GDY exhibited larger electron density around carboxyl group (>0.6 e $Bohr^{-3}$) than that of hydrophobic one (0.4 e $Bohr^{-3}$), indicating superhydrophilic GDY is beneficial to electrostatic assembly with positively charged CoAL-LDH (CO_3^{2-}) nanosheets. The smaller distance and more negative adhesive energies (E_a) between superhydrophilic GDY and CoAl-LDH suggested stronger chemical and electronic interaction than those in hydrophobic CoAl-LDH/GDY (Figure 4c,f). Moreover, the H_2O molecules were closer to the superhydrophilic GDY (Figure 4d, 4g), and the superhydrophilicity could gather H_2O molecules around catalysts to promote interfacial mass/electron transfer (Figure 4e,h). Altogether, the superior electrocatalytic activity of superhydrophilic CoAl-LDH/GDY is derived from the multiple advantages that occurred at superhydrophilic GDY: 1) the more negative charge density is

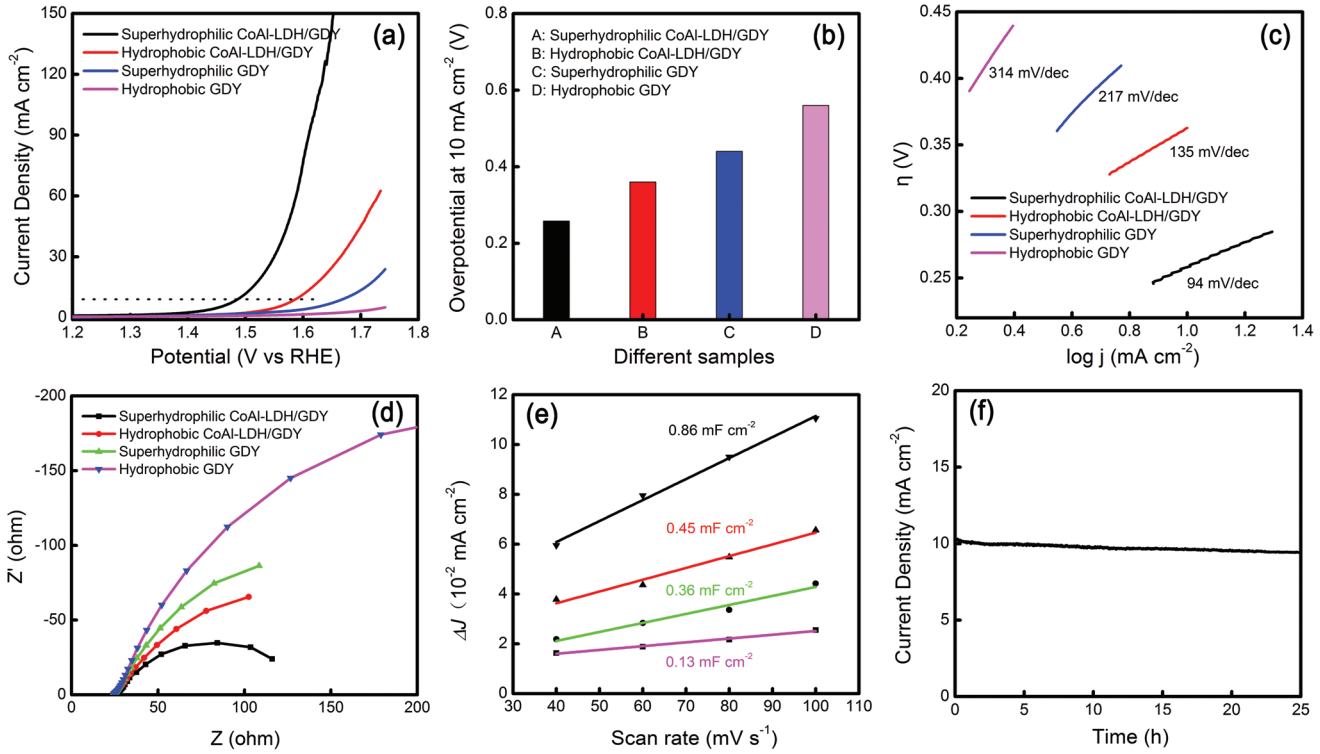

Figure 3. a) LSV curves of hydrophobic GDY, superhydrophilic GDY, hydrophobic CoAl-LDH/GDY, and superhydrophilic CoAl-LDH/GDY electrodes in 0.1 M KOH; b) required overpotential to reach 10 mA cm^{-2} of the different samples; c) Tafel plots of the different samples; d) Nyqyist plots of the corresponding electrodes; e) double-layer capacitance per geometric; f) long-time stability test for superhydrophilic CoAl-LDH/GDY electrode.

beneficial to the electrostatic assembly with positively charged CoAl-LDH, thus improving the loading mass of catalyst; 2) the stronger interaction between superhydrophilic GDY and CoAl-LDH facilitated the formation of CoAl-LDH/GDY hybrid, thus promoting rapid electron transfer from catalysts to GDY; 3) the superhydrophilicity attracted water molecules closer to catalysts to make electrolyte–catalysts contact sufficiently, thus accelerating interfacial mass and electron transport.

To examine the generality of superhydrophilic GDY for water splitting, we extended the fabrication to photoelectrochemical cell. $BiVO_4$ is regarded as one of the most promising photoanode materials for OER, because of its proper bandgap, excellent light absorption ability, and low cost of synthesis.[24,25] However, the OER performance was limited by its high electron-hole recombination and poor water oxidation kinetics. Herein, GDY/$BiVO_4$ synthesized by copper envelope method was treated by air-plasma and then immersed into the ultrathin CoAl-LDH (CO_3^{2-}) colloid to anchor catalysts. EDS and XPS spectra confirmed the successful assembly of catalysts on GDY/$BiVO_4$ surface (Figure S13–S14, Supporting Information). The highest occupied molecular orbital (HOMO) level of superhydrophilic GDY (≈2.0 V vs NHE) located between the valance band (VB) of $BiVO_4$ and the redox potential of CoAL-LDH (Figure S15, Supporting Information), making superhydrophilic GDY play a role of charge mediator to transfer holes from $BiVO_4$ to catalyst (Figure S16, Supporting Information). The photoluminescence (PL) emission spectra and electrochemical impedance spectra were performed to characterize the separation, migration, and transfer of photogenerated electron-hole pairs. As shown in **Figure 5**a, the PL intensity of superhydrophilic GDY/$BiVO_4$ decreased slightly compared with that of hydrophobic GDY/$BiVO_4$ and the superhydrophilic CoAl-LDH/GDY/$BiVO_4$ declined maximally, indicating that the integrated contribution of superhydrophilic GDY and CoAl-LDH facilitated the charge separation remarkably. The charge carrier density of hydrophobic GDY/$BiVO_4$, superhydrophilic GDY/$BiVO_4$, hydrophobic CoAl-LDH/GDY/$BiVO_4$, and superhydrophilic CoAl-LDH/GDY/$BiVO_4$ was further calculated as 2.94×10^{20}, 3.81×10^{20}, 2.97×10^{20}, and 3.85×10^{20} by Mott–Schottky equation, respectively (Figure 5b). The very slight change indicated that plasma treatment and CoAl-LDH assembly had little affect on the charge carrier density of original electrode. By extrapolating the Mott–Schottky plot to *x*-axis, the flat band potential exhibited the most positive shift for superhydrophilic CoAl-LDH/GDY/$BiVO_4$, suggesting a decrease in the bending of the band edges, which is beneficial to the electrode/electrolyte interface charge transfer.[26]

The photoelectrochemical (PEC) performance was carried out in 0.1 M Na_2SO_4 solution with a three-electrode system. As shown in Figure 5c, all of the samples with negligible current in dark (Figure S17, Supporting Information) exhibited obvious photocurrent under illumination of 100 mW cm^{-2} Xe lamp. As expected, the superhydrophilic CoAl/GDY/$BiVO_4$ generated the highest photocurrent of ≈3.15 mA cm^{-2} at 1.23 V versus RHE among the four samples. The half-cell photoconversion efficiency of superhydrophilic CoAl/GDY/$BiVO_4$ electrode reached 0.63% (Figure 5d), which is higher than other LDH-based $BiVO_4$ photoanodes

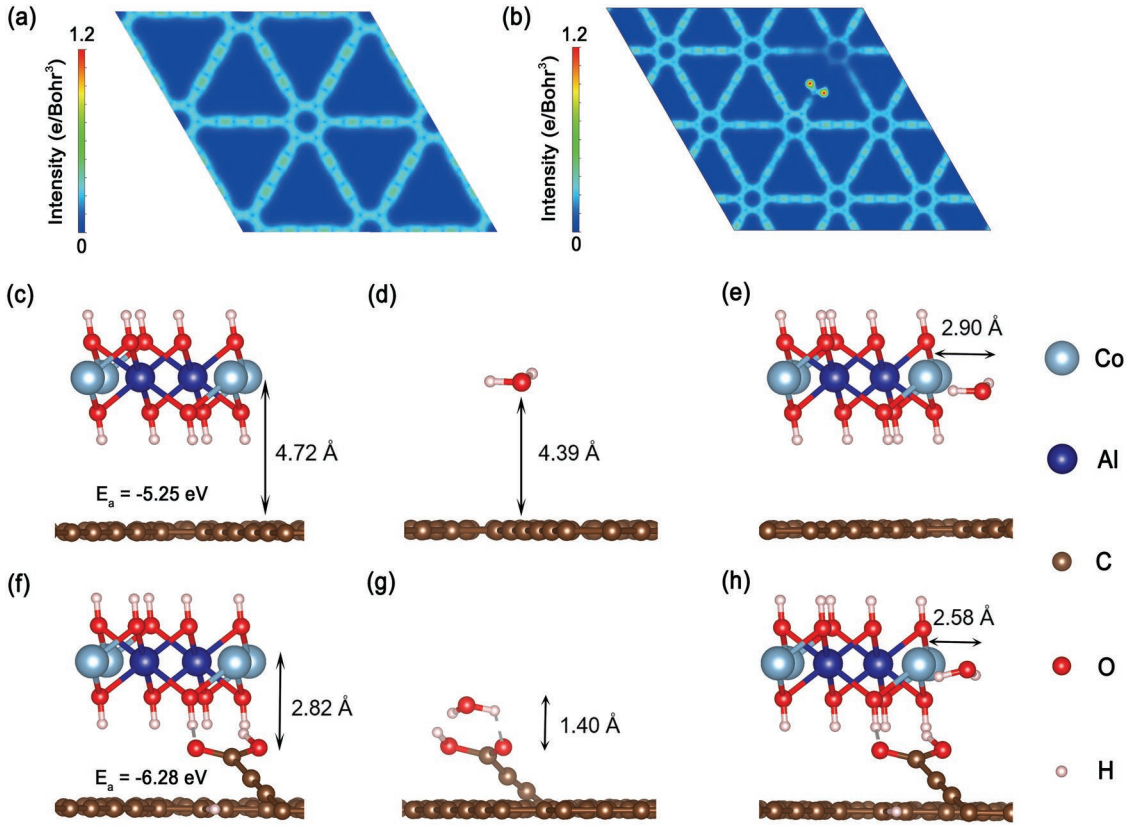

Figure 4. Electron density mapping of a) hydrophobic GDY and b) superhydrophilic GDY; the optimized configuration of c) hydrophobic CoAl-LDH/GDY and f) superhydrophilic CoAl-LDH/GDY; the optimized configuration between H_2O molecules and d) hydrophobic GDY, g) superhydrophilic GDY; the optimized configuration between H_2O molecule and e) hydrophobic CoAl-LDH/GDY, h) superhydrophilic CoAl-LDH/GDY.

(Table S2, Supporting Information). All the samples exhibited the maximum incident photo-to-current conversion efficiency (IPCE) at ≈420 nm and superhydrophilic CoAl-LDH/GDY/$BiVO_4$ exhibited the best value, reaching up to ≈50% (Figure 5e). All the IPCE curves started photoresponse at ≈525 nm, consistent with the UV–visible diffusion absorbance spectra (Figure S18, Supporting Information). Clearly, the plasma treatment and CoAl-LDH assembly barely affect the adsorption of original electrode. During 8 h photoelectrolysis, the superhydrophilic CoAl-LDH/GDY/$BiVO_4$ electrode kept relatively stable photocurrent (Figure 5f) and the faradic efficiency was calculated to be ≈94% and ≈97% for oxygen and hydrogen production, respectively (Figure S19, Supporting Information). These results revealed that superhydrophilic GDY could also be applied to improve the PEC activity largely.

3. Conclusions

In conclusion, we have fabricated the first superhydrophilic GDY electrode via air-plasma treatment and assembled ultrathin CoAl-LDH (CO_3^{2-}) nanosheets onto the surface via electrostatic interaction. The prepared superhydrophilic CoAl-LDH/GDY displays excellent OER activity with an overpotential of ≈258 mV to reach 10 mA cm^{-2}. The TOF was calculated to be ≈0.60 s^{-1} at η = 300 mV, which is one of the best records in LDH-based electrocatalysts. DFT calculations revealed that the superior activity is due to the advantages of superhydrophilic GDY, including the increased electron density, enhanced interactions with catalysts, and improved interfacial mass/electron transfer. The fabrication method has been extended to superhydrophilic CoAl-LDH/GDY/$BiVO_4$ photoanode, leading to an improved photoelectrocatalytic performance. The superhydrophilic CoAl-LDH/GDY is but one example to show the superiority of superhydrophilic GDY in fabricating GDY-based catalytic system for water splitting, which opens a new avenue for GDY in water splitting and provides meaningful information to construct superwettable electrode for gas-involved reactions.

4. Experimental Section

Preparation of Ultrathin CoAl-LDH (CO_3^{2-}) Nanosheets: Ultrathin CoAl-LDH (CO_3^{2-}) nanosheets were prepared as follows.[16] Typically, 0.8 mmol of $Co(NO_3)_2{\cdot}6H_2O$, 0.4 mmol of $Al(NO_3)_3{\cdot}9H_2O$, and 2.8 mmol of urea were put into a 100 mL Teflonlined autoclave containing 80 mL of ethylene glycol, and heated at 100 °C for 24 h. After cooled to room temperature, the suspension was centrifuged to get the paste sample and washed by ethanol for three times. Then, the sample was sonicated in water for 12 h. Then, the obtained pink colloidal suspension was centrifuged at 3000 rpm for 10 min to remove the unexfoliated LDH. The supernatant

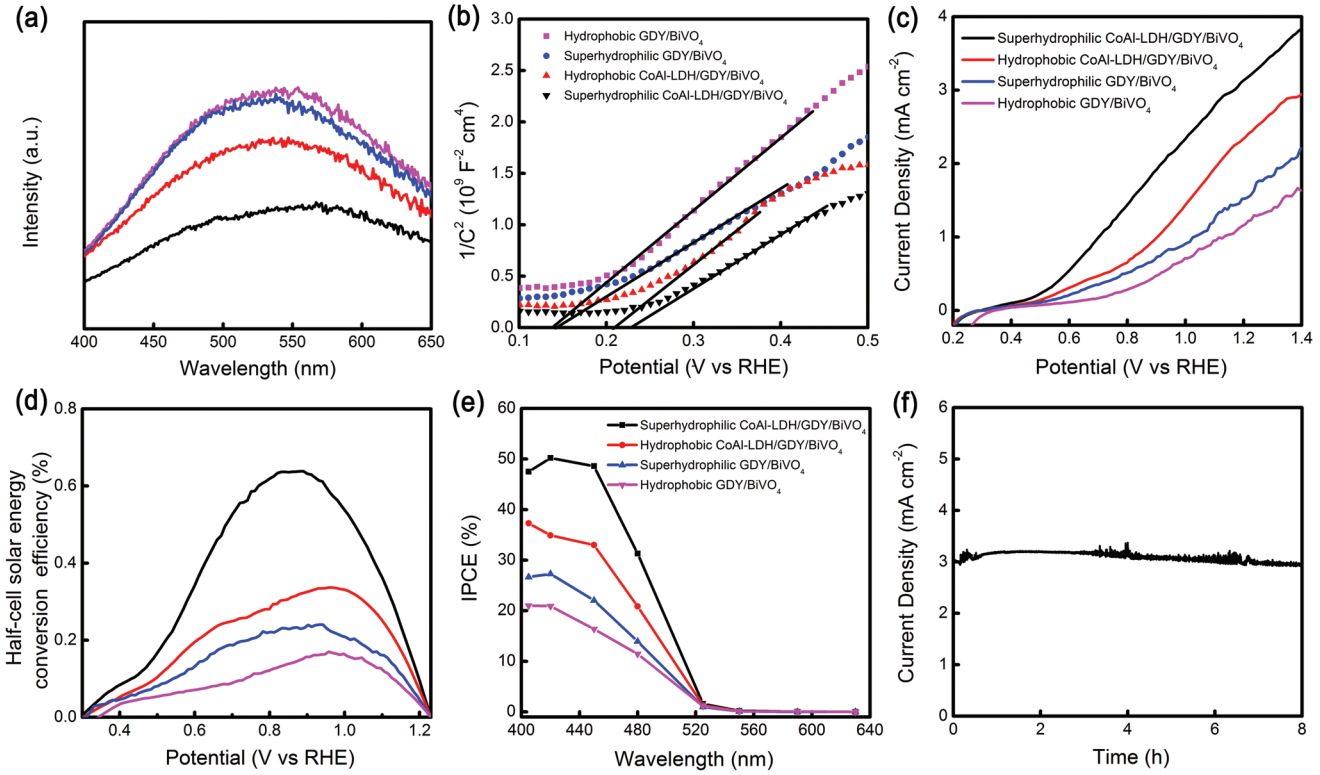

Figure 5. a) Photoluminescence (PL) emission spectra of different samples (the colors were in line with below pictures); b) Mott–Schottky plots measured at the frequency of 1 kHz in dark; c) LSV curves and d) corresponding half-cell solar energy conversion efficiency for the superhydrophilic GDY/$BiVO_4$, CoAl-LDH/GDY/$BiVO_4$, hydrophobic GDY/$BiVO_4$, and CoAl-LDH/GDY/$BiVO_4$ electrodes under 100 mW cm^{-2} Xe lamp illumination; e) IPCEs measured at 1.23 V versus RHE; f) stability test of superhydrophilic CoAl-LDH/GDY/$BiVO_4$ electrode at 1.23 V versus RHE under illumination.

containing LDH nanosheets was collected and used for following experiments.

Preparation of Superhydrophilic GDY and CoAl-LDH/GDY Electrode: Hydrophobic GDY was synthesized on Cu foam by a modified Hay–Glaser coupling reaction.[6] Then the hydrophobic GDY was treated by the air-plasma cleaner for 10 min to obtain the superhydrophilic GDY. The superhydrophilic CoAl-LDH/GDY electrode was prepared by immersing the superhydrophilic GDY electrode into ultrathin CoAl-LDH colloidal suspension for 6 h. Then it was washed by deionized water and dried under a flow of argon.

Preparation of GDY/$BiVO_4$ and CoAl-LDH/GDY/$BiVO_4$ Electrodes: The GDY/$BiVO_4$ electrodes were prepared according to our previous reported literatures.[10c] Then the GDY/$BiVO_4$ electrode was treated by air-plasma to modify the wettability. Afterward, the superhydrophilic GDY/$BiVO_4$ was immersed in the ultrathin CoAl-LDH (CO_3^{2-}) colloidal suspension for 6 h and was dried under a flow of argon.

Supporting Information

Supporting Information is available from the Wiley Online Library or from the author.

Acknowledgements

This work was supported by the Ministry of Science and Technology of China (2017YFA0206903, 2016YFA0200104, and 2014CB239402), the National Natural Science Foundation of China (91427303, 21861132004, and 51432002), the Strategic Priority Research Program of the Chinese Academy of Science (XDB17000000), Key Research Program of Frontier Sciences of the Chinese Academy of Science (QUZDY-SSW-JSC029), and K. C. Wong Education Foundation.

Conflict of Interest

The authors declare no conflict of interest.

Keywords

electrocatalysis, photoelectrocatalysis, superhydrophilic graphdiyne, water oxidation

Received: November 14, 2018
Revised: December 28, 2018
Published online: January 31, 2019

[1] a) Z. Jia, Y. Li, Z. Zuo, H. Liu, C. Huang, Y. Li, *Acc. Chem. Res.* **2017**, *50*, 2470; b) Y. Li, L. Xu, H. Liu, Y. Li, *Chem. Soc. Rev.* **2014**, *43*, 2572.

[2] a) J. Zhou, X. Gao, R. Liu, Z. Xie, J. Yang, S. Zhang, G. Zhang, H. Liu, Y. Li, J. Zhang, Z. Liu, *J. Am. Chem. Soc.* **2015**, *137*, 7596; b) G. Li, Y. Li, H. Liu, Y. Guo, Y. Li, D. Zhu, *Chem. Commun.* **2010**, *46*, 3256.

[3] a) Z.-Z. Lin, *Carbon* **2016**, *108*, 343; b) M. Long, L. Tang, D. Wang, Y. Li, Z. Shuai, *ACS Nano* **2011**, *5*, 2593.
[4] a) S. Wang, L. Yi, J. E. Halpert, X. Lai, Y. Liu, H. Cao, R. Yu, D. Wang, Y. Li, *Small* **2012**, *8*, 265; b) H. Qi, P. Yu, Y. Wang, G. Han, H. Liu, Y. Yi, Y. Li, L. Mao, *J. Am. Chem. Soc.* **2015**, *137*, 5260.
[5] a) H. Shang, Z. Zuo, L. Li, F. Wang, H. Liu, Y. Li, Y. Li, *Angew. Chem., Int. Ed.* **2018**, *57*, 774; b) S. Zhang, H. Du, J. He, C. Huang, H. Liu, G. Cui, Y. Li, *ACS Appl. Mater. Interfaces* **2016**, *8*, 8467.
[6] X. Gao, J. Zhou, R. Du, Z. Xie, S. Deng, R. Liu, Z. Liu, J. Zhang, *Adv. Mater.* **2016**, *28*, 168.
[7] a) M. Li, Z.-K. Wang, T. Kang, Y. Yang, X. Gao, C.-S. Hsu, Y. Li, L.-S. Liao, *Nano Energy* **2018**, *43*, 47; b) Z. Jin, M. Yuan, H. Li, H. Yang, Q. Zhou, H. Liu, X. Lan, M. Liu, J. Wang, E. H. Sargent, Y. Li, *Adv. Funct. Mater.* **2016**, *26*, 5284.
[8] a) Y.-Y. Han, X.-L. Lu, S.-F. Tang, X.-P. Yin, Z.-W. Wei, T.-B. Lu, *Adv. Energy Mater.* **2018**, *8*, 1870077; b) J. Li, X. Gao, B. Liu, Q. Feng, X.-B. Li, M.-Y. Huang, Z. Liu, J. Zhang, C.-H. Tung, L.-Z. Wu, *J. Am. Chem. Soc.* **2016**, *138*, 3954.
[9] a) H. Yu, Y. Xue, L. Hui, C. Zhang, Y. Zhao, Z. Li, Y. Li, *Adv. Funct. Mater.* **2018**, *28*, 1707564; b) Y. Xue, Y. Guo, Y. Yi, Y. Li, H. Liu, D. Li, W. Yang, Y. Li, *Nano Energy* **2016**, *30*, 858; c) Y. Xue, B. Huang, Y. Yi, Y. Guo, Z. Zuo, Y. Li, Z. Jia, H. Liu, Y. Li, *Nat. Commun.* **2018**, *9*, 1460.
[10] a) J. Li, X. Gao, X. Jiang, X.-B. Li, Z. Liu, J. Zhang, C.-H. Tung, L.-Z. Wu, *ACS Catal.* **2017**, *7*, 5209; b) Y. Xue, Z. Zuo, Y. Li, H. Liu, Y. Li, *Small* **2017**, *13*, 1700936; c) X. Gao, J. Li, R. Du, J. Zhou, M. Y. Huang, R. Liu, J. Li, Z. Xie, L. Z. Wu, Z. Liu, J. Zhang, *Adv. Mater.* **2017**, *29*, 1605308.
[11] a) Z. W. Seh, J. Kibsgaard, C. F. Dickens, I. Chorkendorff, J. K. Norskov, T. F. Jaramillo, *Science* **2017**, *355*, eaad4998; b) Y. Jiao, Y. Zheng, M. Jaroniec, S. Z. Qiao, *Chem. Soc. Rev.* **2015**, *44*, 2060; c) Q. Yun, Q. Lu, X. Zhang, C. Tan, H. Zhang, *Angew. Chem., Int. Ed.* **2018**, *57*, 626; d) M. G. Walter, E. L. Warren, J. R. McKone, S. W. Boettcher, Q. Mi, E. A. Santori, N. S. Lewis, *Chem. Rev.* **2010**, *110*, 6446.
[12] a) L. Yu, H. B. Wu, X. W. Lou, *Acc. Chem. Res.* **2017**, *50*, 293; b) M. S. Faber, S. Jin, *Energy Environ. Sci.* **2014**, *7*, 3519; c) F. E. Osterloh, *Chem. Soc. Rev.* **2013**, *42*, 2294; d) Y. P. Zhu, C. Guo, Y. Zheng, S.-Z. Qiao, *Acc. Chem. Res.* **2017**, *50*, 915.
[13] a) P. Wang, T. Hayashi, Q. Meng, Q. Wang, H. Liu, K. Hashimoto, L. Jiang, *Small* **2017**, *13*, 1601250; b) C. Tang, H. F. Wang, Q. Zhang, *Acc. Chem. Res.* **2018**, *51*, 881; c) Z. Lu, W. Zhu, X. Yu, H. Zhang, Y. Li, X. Sun, X. Wang, H. Wang, J. Wang, J. Luo, X. Lei, L. Jiang, *Adv. Mater.* **2014**, *26*, 2683.
[14] a) Y. Li, H. Zhang, T. Xu, Z. Lu, X. Wu, P. Wan, X. Sun, L. Jiang, *Adv. Funct. Mater.* **2015**, *25*, 1737; b) W. Xu, Z. Lu, X. Sun, L. Jiang, X. Duan, *Acc. Chem. Res.* **2018**, *51*, 1590; c) J. He, B. Hu, Y. Zhao, *Adv. Funct. Mater.* **2016**, *26*, 5998.
[15] J. Ping, Y. Wang, Q. Lu, B. Chen, J. Chen, Y. Huang, Q. Ma, C. Tan, J. Yang, X. Cao, Z. Wang, J. Wu, Y. Ying, H. Zhang, *Adv. Mater.* **2016**, *28*, 7640.
[16] H. Li, T. N. Tran, B. J. Lee, C. Zhang, J. D. Park, T. H. Kang, J. S. Yu, *ACS Appl. Mater. Interfaces* **2017**, *9*, 20294.
[17] P. Kuang, B. Zhu, Y. Li, H. Liu, J. Yu, K. Fan, *Nanoscale Horiz.* **2018**, *3*, 317.
[18] G. Shi, C. Yu, Z. Fan, J. Li, M. Yuan, *ACS Appl. Mater. Interfaces* **2018** https://doi.org/10.1021/acsami.8b03345.
[19] F. Song, X. Hu, *J. Am. Chem. Soc.* **2014**, *136*, 16481.
[20] X. Long, J. Li, S. Xiao, K. Wang, H. Chen, S. Yang, *Angew. Chem., Int. Ed.* **2014**, *53*, 7584.
[21] a) H. Wang, L. Zhang, Z. Chen, J. Hu, S. Li, Z. Wang, J. Liu, X. Wang, *Chem. Soc. Rev.* **2014**, *43*, 5234; b) J. D. Blakemore, R. H. Crabtree, G. W. Brudvig, *Chem. Rev.* **2015**, *115*, 12974; c) L. Duan, F. Bozoglian, S. Mandal, B. Stewart, T. Privalov, A. Llobet, L. Sun, *Nat. Chem.* **2012**, *4*, 418.
[22] a) P. Zhang, T. Wang, J. Gong, *Chem* **2018**, *4*, 223; b) J. R. Swierk, T. E. Mallouk, *Chem. Soc. Rev.* **2013**, *42*, 2357; c) W. Liu, H. Liu, L. Dang, H. Zhang, X. Wu, B. Yang, Z. Li, X. Zhang, L. Lei, S. Jin, *Adv. Funct. Mater.* **2017**, *27*, 1603904.
[23] a) H. Yan, S. Guo, F. Wu, P. Yu, H. Liu, Y. Li, L. Mao, *Angew. Chem., Int. Ed.* **2018**, *57*, 3922; b) L. D'Urso, G. Forte, P. Russo, C. Caccamo, G. Compagnini, O. Puglisi, *Carbon* **2011**, *49*, 3149.
[24] a) T. W. K. K.-S. Choi, *Science* **2014**, *343*, 990; b) M. Zhong, T. Hisatomi, Y. Kuang, J. Zhao, M. Liu, A. Iwase, H. Nishiyama, C. Katayama, H. Shibano, M. Katayama, A. Kudo, T. Yamada, K. Domen, *J. Am. Chem. Soc.* **2015**, *137*, 5053.
[25] a) K.-H. Ye, Z. Wang, J. Gu, S. Xiao, Y. Yuan, Y. Zhu, Y. Zhang, W. Mai, S. Yang, *Energy Environ. Sci.* **2017**, *10*, 772; b) S. Ye, C. Ding, R. Chen, F. Fan, P. Fu, H. Yin, X. Wang, Z. Wang, P. Du, C. Li, *J. Am. Chem. Soc.* **2018**, *140*, 3250.
[26] a) F. Ning, M. Shao, S. Xu, Y. Fu, R. Zhang, M. Wei, D. G. Evans, X. Duan, *Energy Environ. Sci.* **2016**, *9*, 2633; b) W. Li, P. Da, Y. Zhang, Y. Wang, X. Lin, X. Gong, G. Zheng, *ACS Nano* **2014**, *8*, 11770.